PROCEEDINGS, 47th Workshop on Geothermal Reservoir Engineering
Stanford University, Stanford, California, February 7-9, 2022
SGP-TR-223

Techno-Economic Study of Separated Brine Heat Recovery Using Bottoming Organic Rankine Cycle in Lumut Balai Geothermal Power Plant, Indonesia

Vincentius Adven Brilian[1], Fikri Muhammad Akbar[1], Resa Wardana Saputra[2]

[1]Department of Mechanical and Industrial Engineering, Universitas Gadjah Mada, Jl. Grafika No. 2, Yogyakarta, Indonesia 55281

[2]Department of Chemical Engineering, Universitas Gadjah Mada, Jl. Grafika No. 2, Yogyakarta, Indonesia 55281

adven.brilian01@mail.ugm.ac.id

Keywords: bottoming Organic Rankine Cycle, economic analysis, energy analysis, separated brine, scaling

ABSTRACT

A single unit of geothermal power plant (GPP) with an installed capacity of 1x55 MW was commissioned in Lumut Balai geothermal field in 2019. The field is a liquid-dominated geothermal system with a reservoir temperature of around 240°C. Lumut Balai GPP disposed 2204.6 tonne/h of separated brine at a temperature of 164.9°C into the hot brine reinjection wells without further utilization. In this study, a bottoming power plant using Organic Rankine Cycle (ORC) is proposed to recover heat from the separated brine to generate more electricity. The proposed bottoming ORC is analyzed using the techno-economic approach, consisting of technical and economic analyses. The technical analysis is conducted using energy analysis with the aid of Engineering Equation Solver (EES) to study the system's technical performance (net power output and thermal efficiency). The optimization is performed by varying the working fluid and the turbine inlet pressure. Three working fluids are used in this study, namely n-pentane, n-butane, and isobutene. The measured silica concentration in the separated brine is 600 ppm. Using the silica saturation index (SSI) of 1.0 as a silica scaling potential indicator, the temperature of the separated brine is maintained above 146°C to prevent scaling. The energy analysis result shows that the bottoming ORC can yield the highest net power output and thermal efficiency of 13,215 kW and 26.1%, respectively, using n-pentane as the working fluid. Furthermore, economic analysis is performed to study the feasibility of the system using Internal rate of return (IRR), net present value (NPV), and payback period as the indicators. The result shows that the system is economically feasible with an IRR of 18%, an NPV of 66.3 million USD, and a payback period of 7.3 years.

1. INTRODUCTION

With the rise of global energy demands, fossil fuels as energy sources will inevitably run out, forcing us to somehow switch to the currently developed renewable energy sources. Geothermal energy as one of the highly-rated potential sources to replace fossil fuels will go accordingly with 2015's Paris Agreement objectives, which is to reduce global greenhouse gas emissions by 40% in 2030. It will also help Indonesia in reaching the country's target of mixed energy, which stated that 23% of energy will be generated by renewable sources by 2025. With the country's location located in the ring of fire, Indonesia has approximately 29 GW of geothermal energy scattered across the archipelago. But with this much potential, the usage is still relatively small with only 2130.7 MW installed electric capacity generated from the 16 power plants across the country (Hidayah et al., 2020).

Lumut Balai geothermal power plant (GPP) is located in the village of Penandaian, South Sumatera province, at least 292 km southwest of Palembang city. The complete project of the GPP includes two phases, the first being the development of Units 1 and 2, then the second for Units 3 and 4 (Sulistyardi, 2015). The production wells are distributed on four wellpads, and two different wellpads are used for reinjection. By 2019, GPP Unit of 1x55 MW capacity was installed in Lumut Balai geothermal field. To be able to optimize the potential power output of this power plant, generating additional electricity by recovering waste heat from the separated geothermal brine can be done by using bottoming binary cycle, which is a relatively optimal method if compared to others. One of the cycles is Organic Rankine Cycle (ORC), where the system will be explained later in this research paper. This research covers the techno-economic analysis of the proposed system, which consists of technical analysis using thermodynamics energy analysis and economic feasibility analysis.

2. METHODOLOGY

2.1 System Description

The waste heat from the separated geothermal brine from the existing Lumut Balai GPP separator is transferred to a bottoming Organic Rankine Cycle (ORC) to generate additional electricity. In this study, basic ORC configuration without recuperator is used, as shown in Figure 1. The high-pressure ORC working fluid leaving the feed pump flows into the preheater to be heated into the saturated liquid phase at evaporator pressure using the waste heat from the separated geothermal brine. Subsequently, the ORC working fluid is changed into a saturated vapor phase inside the evaporator at constant pressure using the waste heat from separated geothermal brine. This saturated vapor turns the ORC turbine to generate electric power. Afterward, the energy-depleted vapor from the ORC turbine is condensed into saturated liquid at 28°C inside the air-cooled condenser (ACC). Later, the ORC working fluid flows into the feed pump again to increase its pressure. Then, the ORC working fluid leaving the feed pump flows into the preheater, and the cycle repeats.

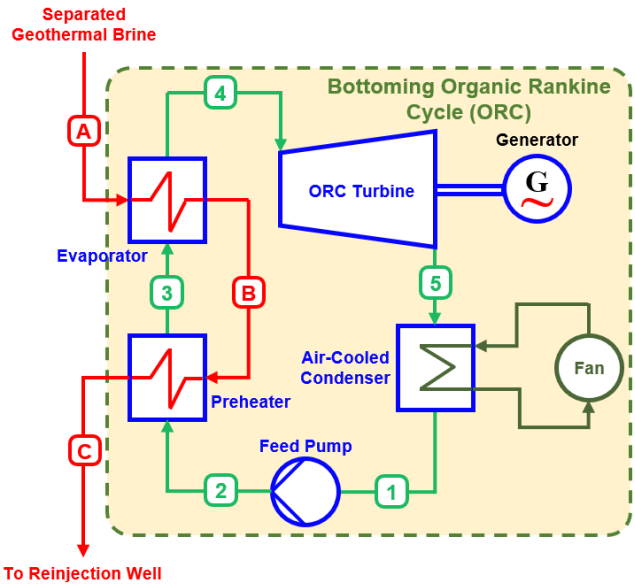

Figure 1: Schematic of basic bottoming Organic Rankine Cycle.

2.2 Technical Analysis

Technical analysis is conducted to design the bottoming ORC with the most optimum performance using thermodynamics energy analysis. The energy balance equations of each component of the bottoming ORC are developed and solved using Engineering Equation Solver (EES). The technical parameters of the bottoming ORC involve geothermal brine and condensate condition from the existing GPP, bottoming ORC equipment basic specification, and ambient condition as shown in Table 1.

Table 1: Technical parameters of the bottoming ORC.

Parameter	Value	Unit	Source
Separated geothermal brine mass flow rate	612.4	kg/s	Sulistyardi (2015)
Separated geothermal brine temperature	164.9	°C	Sulistyardi (2015)
Separated geothermal brine pressure	7	bar	Sulistyardi (2015)
Separated geothermal brine measured silica content	600	ppm	JICA (2011)
Evaporator pinch-point temperature	5	°C	Wakana (2013)
Turbine isentropic efficiency	85	°C	Pambudi et al. (2015)
Condenser temperature	28	%	Wakana (2013)
Ambient temperature	25	°C	Sulistyardi (2015)
Atmospheric pressure	0.8879	bar	Sulistyardi (2015)
Cooling air temperature difference	12	°C	Wakana (2013)
Fan motor efficiency	75	%	Wakana (2013)
Feed pump isentropic efficiency	75	%	Pambudi et al. (2015)

The technical performance indicators analyzed in this study are the specific power output per unit mass flow rate of ORC working fluid and thermal efficiency using three different ORC working fluids, namely n-pentane, n-butane, and isopentane. The properties of each ORC working fluid are shown in Table 2. The system's performance optimization is performed by variating the turbine inlet pressure.

Table 2: Properties of ORC working fluids considered in this study (Hidayah et al., 2020; Wakana, 2013).

Working Fluid	ASHRAE	Chemical Formula	$T_{critical}$ (°C)	$P_{critical}$ (bar)	Global Warming Potential
n-pentane	R-601	C_5H_{12}	196.5	33.75	6
n-butane	R-600	C_4H_{10}	152.0	37.96	4
Isopentane	R-601a	i-C_5H_{12}	187.8	33.78	5

2.2.1 Feed Pump Energy Balance and Efficiency

The energy balance and efficiency for the feed pump are expressed by Equations (1) and (2), respectively, as follows:

$$\dot{W}_{pump} = \dot{m}_{wf}(h_1 - h_5) \quad (1)$$

$$\eta_{pump} = \frac{h_{1s} - h_5}{h_1 - h_5} \quad (2)$$

where $\dot{W}_{pump}$, η_{pump}, $\dot{m}_{wf}$, h_1, h_{1s}, h_5 are required pumping power, pump isentropic efficiency, ORC working fluid mass flow rate, ORC working fluid enthalpy at the pump outlet, ORC working fluid isentropic enthalpy at the pump outlet, and ORC working fluid enthalpy at the pump inlet, respectively.

2.2.2 Preheater Energy Balance

The energy balance for preheater as a result of heat exchange between separated geothermal brine and ORC working fluid is expressed by Equation (3) as follows:

$$\dot{m}_{brine}(h_b - h_c) = \dot{m}_{wf}(h_2 - h_1) \quad (3)$$

where $\dot{m}_{brine}$, $\dot{m}_{wf}$, h_b, h_c, h_1, h_1 are geothermal brine mass flow rate, ORC working fluid mass flow rate, brine mass flow rate at preheater inlet, brine enthalpy at preheater outlet, ORC working fluid enthalpy at preheater inlet, and ORC working fluid enthalpy at preheater outlet, respectively.

2.2.3 Evaporator Energy Balance

The energy balance for evaporator as a result of heat exchange between separated geothermal brine and ORC working fluid is expressed by Equation (4) as follows:

$$\dot{m}_{brine}(h_a - h_b) = \dot{m}_{wf}(h_3 - h_2) \quad (4)$$

where $\dot{m}_{brine}$, $\dot{m}_{wf}$, h_a, h_b, h_2, h_3 are geothermal brine mass flow rate, ORC working fluid mass flow rate, brine enthalpy at the evaporator inlet, brine enthalpy at evaporator outlet, ORC working fluid enthalpy at the evaporator inlet, and ORC working fluid enthalpy at evaporator outlet, respectively.

2.2.4 ORC Turbine Energy Balance and Efficiency

The energy balance and efficiency of the ORC turbine are expressed by Equations (5) and (6), respectively, as follows:

$$\dot{W}_{turbine} = \dot{m}_{wf}(h_3 - h_4) \quad (5)$$

$$\eta_{turbine} = \frac{h_3 - h_4}{h_3 - h_{4s}} \quad (6)$$

where $\dot{W}_{turbine}$, $\eta_{turbine}$, $\dot{m}_{wf}$, h_3, h_4, h_{4s} are turbine power output, turbine isentropic efficiency, ORC working fluid mass flow rate, ORC working fluid enthalpy at turbine inlet, ORC working fluid enthalpy at turbine outlet, and ORC working fluid isentropic enthalpy at turbine outlet, respectively.

2.2.5 Air-Cooled Condenser Energy Balance, Required Power, and Fan Motor Efficiency

The energy balance, required power, and fan motor efficiency of the air-cooled condenser (ACC) are expressed by Equations (7), (8), and (9), respectively, as follows:

$$\dot{m}_{air} c_{p,air}(T_{air,out} - T_{air,in}) = \dot{m}_{wf}(h_4 - h_5) \quad (7)$$

$$\dot{W}_{fan} = \frac{\Delta p \times \dot{m}_{air}}{\rho_{air,out} \times \eta_{fan,motor}} \quad (8)$$

$$\eta_{fan,motor} = \frac{\dot{W}_{fan}}{P_{fan,motor}} \quad (9)$$

where $\dot{m}_{air}$, $\dot{m}_{wf}$, $c_{p,air}$, $T_{air,out}$, $T_{air,in}$, h_4, h_5, $P_{fan,motor}$, Δp, $\rho_{air,out}$, $\dot{W}_{fan}$, $\eta_{fan,motor}$ are cooling air mass flow rate, ORC working fluid mass flow rate, air specific heat at constant pressure, leaving cooling air temperature, incoming cooling air temperature, ORC working fluid enthalpy at condenser inlet, ORC working fluid enthalpy at condenser outlet, fan motor electric power input, fan static head, cooling air density, fan mechanical work, and fan motor efficiency, respectively.

2.2.6 Bottoming ORC Thermal Efficiency

The thermal efficiency of bottoming ORC is expressed by Equation (10) as follows:

$$\eta_{thermal,ORC} = \frac{\dot{W}_{net,out}}{\dot{Q}_{net,in}} = \frac{\dot{W}_{turbine} - (\dot{W}_{pump} + \dot{W}_{fan})}{\dot{m}_{brine}(h_a - h_c)} \quad (10)$$

where $\eta_{thermal,ORC}$, $\dot{W}_{turbine}$, $\dot{W}_{pump}$, $\dot{W}_{fan}$, $\dot{m}_{brine}$, h_a, h_c are bottoming ORC thermal efficiency, turbine power output, required pumping power, fan mechanical work, geothermal brine mass flow rate, brine enthalpy at the evaporator inlet, and brine enthalpy at preheater outlet, respectively.

2.2.7 Silica Saturation Index

Silica Saturation Index (SSI) is used as a silica scaling potential indicator. The separated geothermal brine temperature leaving the bottoming ORC towards the reinjection well should be maintained above the minimum allowable temperature according to SSI in order to prevent silica scaling (Zarrouk and Moun, 2014). The calculation of SSI is expressed by Equation (11). Furthermore, amorphous silica solubility at a specific temperature is expressed by Equation (12), which is valid at the temperature range of 0-250°C (Fournier and Rowe, 1977).

$$SSI = \frac{CI}{C} \quad (11)$$

$$\log C = -\frac{731}{T + 273.15} + 4.52 \quad (12)$$

where *SSI*, *CI*, *C*, *T* are silica scaling index, measured silica concentration, amorphous silica solubility at a specific temperature, and temperature, respectively. In this study, the minimum allowable SSI to prevent silica scaling is 1. Given that the measured silica concentration of the separated geothermal brine is 600 ppm, hence the minimum allowable temperature of the separated geothermal brine leaving the bottoming ORC is 146°C.

2.3 Economic Analysis

2.3.1 Present Value

Present value is the current value of a certain cash flow in the future, which is calculated using a certain interest rate (discount). In general, there are three types of cash flows, the initial outlay is the initial cash outflow, namely investment costs/fixed capital (capital expenditure/CAPEX) , operating (differential) cashflow is the accumulation of cash inflows and outflows that are relevant to the project evaluated during the life of the investment (operational expenditure/OPEX), and terminal cashflow is the final cash flow added to the salvage value/SV and the return on working capital. The present value is expressed in Equation (13) as follows (Sullivan et.al, 2018).

$$PV = \frac{FV}{(1+r)^t} \quad (13)$$

where *PV*, *FV*, *r*, and *t* are present value, future value, discount, and period (year), respectively.

2.3.2 Net Present Value

Net present value (NPV) is the total present value of all project cash flows using a certain discount according to Equation (14) as follows:

$$NPV = -CF_o + \sum \frac{CF_t}{(1+r)^t} \quad (14)$$

where *NPV*, CF_o, CF_t, *r*, and *t* are net present value, cashflow at year-0, cashflow at year-t, discount, and year, respectively. Year-0 cash flow is negative because cash flow is debt in project planning for investment in system equipment to be built. The condition for a project to be declared economically feasible is if the NPV is positive (Bachtiar et al, 2021).

2.3.3 Internal Rate of Return

The internal rate of return (IRR) is the discounted value resulting in the total present value of cash inflows equal to the value of fixed capital (NPV = 0). IRR is expressed in Equation (15):

$$IRR = \frac{CF_t}{(1+IRR)^t} \quad (15)$$

where *IRR*, CF_t, and *t* are internal rate of return, cashflow at year-t, and year, respectively. A project is defined as economically feasible is if the IRR expected return. Expected returns can use rWACC (rate of weighted average cost of capital), which is the average cost of the

debt-to-equity ratio in investment funding. The rWACC value can use the discount as a reference. So, in this case, the project is declared economically feasible if the IRR value is bigger than the discount rate (Achinas & Euverink, 2019).

2.3.4 Payback Period

The payback period states the length of time it takes to return the investment issued. By looking at the payback period, the decision-maker can judge whether a project is worth investing in. The payback period calculation uses Equation (16) as follows:

$$PP = \frac{FC}{NCF} \tag{16}$$

where *PP*, *FC*, and *NCF* are payback period, fixed cost, and net cashflow, respectively.

2.3.5 Economic Assumption

Several assumptions are applied in the calculation which is gathered based on several existing literature as listed in Table 3.

Table 3: Economic parameters used in economic performance calculations.

Parameter	Value
Project lifetime	30 years
Discount rate	10%
Capacity factor	90%
Taxes	25%
Energy price	0.18 USD/kWh
Feed pump price	450 USD/kW
Preheater price	450 USD/kW
Evaporator price	500 USD/kW
ORC turbine price	500 USD/kW
Air-cooled condenser price	400 USD/kW
ACC fan price	400 USD/kW

2.3.6 Economic Modelling

The total investment cost is calculated by following the cost breakdown list suggested by Lemmens (2016), as shown in Table 4.

Table 4: Economic modeling used in economic performance calculations.

Parameter	Percentage	By Component
Direct fixed-capital investments (DFCI)		
Purchased equipment installation	45%	PEC
Piping	31%	PEC
Instrumentation and controls	10%	PEC
Electrical equipment and materials	11%	PEC
Civil, structural, and architectural work	44%	PEC
Service facilities	20%	PEC
Indirect fixed-capital investment (IFCI)		
Engineering and supervision	30%	PEC
Construction costs including contractor's profit	15%	DFCI
Contingencies	10%	FCI
Legal costs	2%	FCI

3. RESULT AND DISCUSSION

3.1 Technical Analysis

The thermodynamics energy analysis is performed using variable turbine inlet pressure using three different ORC working fluids, namely n-pentane, n-butane, and isopentane, in order to achieve a bottoming ORC design with the most optimum performance in terms of thermal efficiency and specific power output. The profile of thermal efficiency and specific power output with respect to turbine inlet pressure using each working fluid are shown in Figure 2. The highest thermal efficiency and specific power output at the lowest turbine inlet pressure are achieved using n-pentane as the ORC working fluid. The important thermodynamics energy analysis results using each ORC working fluid are shown in Table 5.

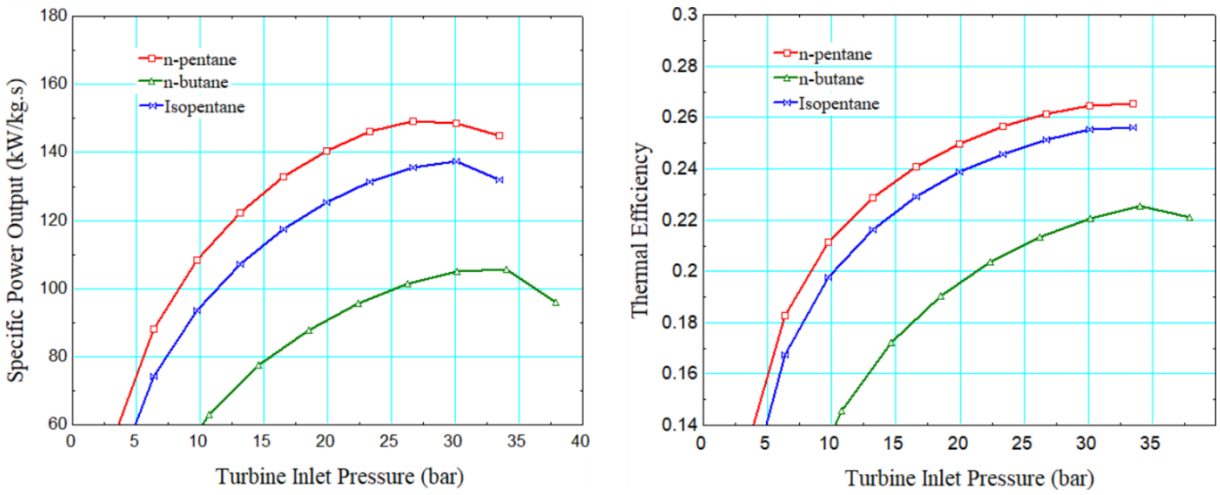

Figure 2: Specific power output vs. turbine inlet pressure (left); Thermal efficiency vs. turbine inlet pressure (right).

Table 5: Important thermodynamics energy analysis parameters of the bottoming ORC.

ORC Working Fluid	Upper Pressure (bar)	Lower Pressure (bar)	Specific Power Output (kW/kg.s)	Thermal Efficiency (%)
n-pentane	26.71	0.769	149.3	26.14
n-butane	34.02	2.673	105.7	22.52
Isopentane	30.11	1.108	131.9	25.51

An example of thermodynamic properties at each state using n-pentane working fluid is shown in Table 6. The optimized bottoming ORC using n-pentane works at a pressure range between 26.71 bar (upper pressure) and 0.769 bar (lower pressure). The saturated n-pentane liquid enters the feed pump (state number 1) at 0.769 bar to increase its pressure to 26.71 bar (state number 2). Afterward, it is preheated at constant pressure using the waste heat from the separated geothermal brine to reach the saturation temperature of 155.4^{o}C at the saturated liquid phase (state number 3). More heat from the separated geothermal brine is transferred to the n-pentane ORC working fluid to change the n-pentane phase from saturated liquid to saturated vapor at constant pressure without changing its temperature (state number 4). The n-pentane then enters the ORC turbine to rotate the turbine-generator unit to generate electricity. Since n-pentane is a dry-type working fluid, it leaves the turbine (state number 5) in the phase of superheated vapor (Nandaliarsyad et al., 2020). The superheated n-pentane vapor is then cooled to the temperature of 28^{o}C and condensed into saturated liquid at the lower pressure of 1.02 bar (state number 1) in the air-cooled condenser. Meanwhile, the saturated liquid geothermal brine from the existing Lumut Balai GPP separator changes its phase into compressed liquid after transferring its heat to evaporate the ORC working fluid. The geothermal brine temperature keeps decreasing as it transfers its heat to preheat the ORC working fluid. The T-s diagram of the optimized bottoming ORC using n-pentane is shown in Figure 3.

Table 6: Thermodynamics properties at each state using n-pentane working fluid.

Parameter	Unit	State							
		A	B	C	1	2	3	4	5
Pressure	bar	7	7	7	0.769	26.71	26.71	26.71	0.769
Temperature	^{o}C	164.9	160.4	146	28	28.87	155.4	155.4	71.39
Vapor quality	-	0	-	-	-	0	1	-	0
Phase	-	Saturated liquid	Compressed liquid	Compressed liquid	Compressed liquid	Saturated liquid	Saturated vapor	Superheated vapor	Saturated liquid
Enthalpy	kJ/kg	697.14	677.36	615.17	4.87	10.51	443.3	581.6	423.4
Entropy	kJ/kg-K	1.992	1.943	1.801	0.0184	0.0184	1.164	1.486	1.486

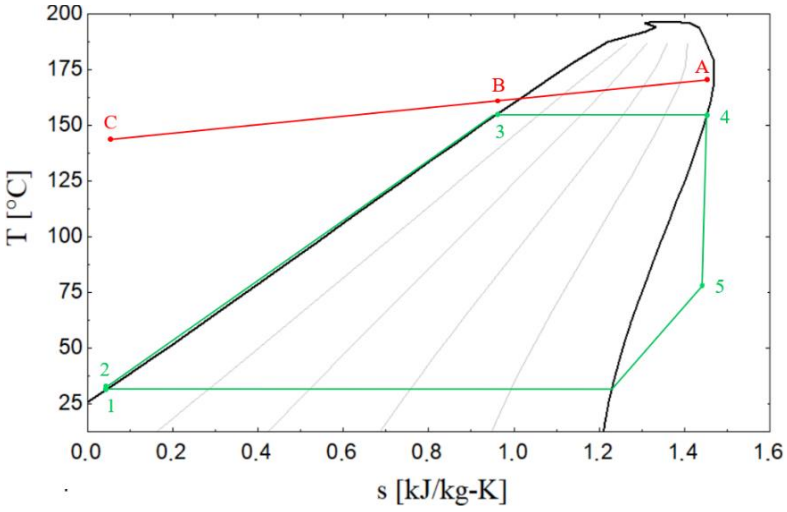

Figure 3: T-s diagram of the bottoming ORC using n-pentane working fluid.

The power output and consumption of the bottoming ORC are shown in Table 7. It can be seen that using n-pentane as the ORC working fluid generates the highest power output from the turbine compared to using n-butane and isopentane. Furthermore, the total house load from the pump and fan power is the lowest when n-pentane is used as the working fluid. Therefore, n-pentane yields the highest net power output of 13,215 kW compared to n-butane and isopentane with net power outputs of 11,387 kW and 12,902 kW, respectively. Additionally, the use of n-pentane requires the least mass flow rate of the working fluid, as much as 88.51 kg/s, compared to n-butane and isopentane with the working fluid mass flow rates of 107.7 kg/s and 93.84 kg/s.

Table 7: Bottoming ORC power output and input using each ORC working fluid.

Parameter	n-pentane	n-butane	Isopentane	Unit
Turbine power output	14,009	12,484	13,793	kW
Pumping power input	499.6	788	593.9	kW
Fan power input	294.9	309.4	297.4	kW
Total house load	794.5	1,097.4	891.3	kW
Net power output	13,215	11,387	12,902	kW
Daily electrical energy production	317.16	273.29	309.65	MWh/day
ORC working fluid mass flow rate	88.51	107.7	93.84	kg/s

3.2 Economic Analysis

We analyze the economic feasibility for n-pentane because n-pentane is the selected working fluid based on thermodynamic analysis. By using predefined economic modeling and parameters, and by considering the value of money that changes over time and is based on investments that do not return at the end of the year during the life of the system, we also calculate the depreciation using the straight-line method with assumption factory economic life (N) is 30 years, annual profit and constant tax, salvage value of 10% of fixed capital. The results of this economic analysis are the amount of internal rate of return (IRR), net present value (NPV), and payback period.

Table 8: Summary of economic feasibility of n-pentane ORC working fluid.

Parameter	Value
Purchased equipment cost	35,680,500 USD
Direct fixed-capital investments (DFCI)	57,445,605 USD
Indirect fixed-capital investment (IFCI)	30,496,123 USD
Total investment	123,622,228 USD
Depreciation	2,793,783 USD
Salvage value	9,312,610 USD
Internal rate of return (IRR)	18%
Net present value (NPV)	66,336,279 USD
Payback period	7.33 years

The results in Table 8 show that the internal rate of return (IRR) is 18%. This result is greater than the discount rate (10%), the net present value is positive, reaching 66 million USD, and the payback period will be reached in 7.3 years with an assumption that the system's lifetime is 30 years. Therefore, the economic analysis of n-pentane as a working fluid in the ORC system is economically feasible.

4. CONCLUSION

A bottoming power plant using Organic Rankine Cycle (ORC) is proposed to recover heat from the separated brine of the existing Lumut Balai Geothermal Power Plant to generate more electricity. Using the silica saturation index (SSI) of 1.0 as a silica scaling potential indicator, the temperature of the separated brine is maintained above 146^{o}C to prevent scaling. The energy analysis result shows that the bottoming ORC can yield the highest net power output and thermal efficiency of 13,215 kW and 26.1%, respectively, using n-pentane as the working fluid. Furthermore, the economic analysis result shows that the system is economically feasible with an IRR of 18%, an NPV of 66.3 million USD, and a payback period of 7.3 years.

REFERENCES

Achinas, S., & Euverink, G.J.W. (2019). Feasibility Study of Biogas Production from Hardly Degradable Material in Co-Inoculated Bioreactor. *Energies*, 12(6). https://doi.org/10.3390/en12061040

Bachtiar, A.Y., Annas, A.C., Fajrin, A.N.A., Rizwan, M.H., & Kartikasari, I.R. (2021). Techno-Economic and Feasibility Assessment of Cryogenic Distillation Membrane for Purification Natural Gas from CO_2. *Indonesian Journal of Energy*. https://doi.org/10.33116/ije.v4i1.102

Fournier, R. O., & Rowe, J. J. (1977). The Solubility of Amorphous and High Pressures Silica in Water at High Temperatures. *American Mineralogist, 62*, 1052–1056.

Hidayah, A. N., Putera, A. D. P, & Subiantoro, A. (2020). Selection of Optimum Working Fluid and Cycle Configuration of Organic Rankine Cycle (ORC) as Bottoming Binary Cycle at Wayang Windu Geothermal Power Plant. *Proceedings 45th Workshop on Geothermal Reservoir Engineering*. Stanford: Stanford University.

Japan International Cooperation Agency (2011). JICA Preparatory Survey for Lumut Balai Geothermal Power Plant Development Project Final Report. Jakarta: JICA.

Lemmens, S. (2016). Cost Engineering Techniques & Their Applicability for Cost Estimation of Organic Rankine Cycle Systems. *Energies*, 9(7). https://doi.org/10.3390/en9070485

Nandaliarasyad, N., Maulana, D.T, Darmanto, P. S. 2020, Study of Development Scenarios for Bottoming Unit Binary Cycle to Utilize Exhaust Steam from Back Pressure Turbine Geothermal Power Plant. *IOP Conference Series: Earth and Environmental Science, 417, 012017*. https://doi.org/10.1088/1755-1315/417/1/ 012017.

Pambudi, N. A., Itoi, R., Jalilinasrabady, S., & Sirait, P. (2015). Preliminary Analysis of Single Flash Combined with Binary System Using Thermodynamic Assessment: A Case Study of Dieng Geothermal Power Plant. *International Journal of Sustainable Engineering, 7038*. https://doi.org/10.1080/19397038.2014.915895

Sulistyardi, H. B. (2015). An Update on the Basic Design of Lumut Balai Geothermal Power Plant, Indonesia. *Proceedings World Geothermal Congress 2015*. Melbourne: International Geothermal Association.

Sullivan, W.G., Wicks, E.M. & Koelling, P.C. (2018). Engineering Economy (17th ed.). New Jersey: Pearson Education.

Wakana, F. (2013). Preliminary Study of Binary Power Plant Feasibility Comparing ORC and Kalina for Low-Temperature Resources in Rusizi Valley, Burundi. *Geothermal Training Programme*. Reykjavik: United Nations University.

Zarrouk, S. J., & Moon, H. (2014). The Efficiency of Geothermal Power Plants: A Worldwide Review. *Geothermics, 51*, 142–153. https://doi.org/10.1016/j.geothermics.2013.11.001